

## ALIASING IN HUMAN FOVEAL VISION

DAVID R. WILLIAMS

Center for Visual Science, University of Rochester, Rochester, NY 14627, U.S.A.

(Received 4 September 1984)

**Abstract**—An improved laser interferometer allows forced choice contrast sensitivity measurements that are relatively unaffected by optical blurring in the eye. At spatial frequencies above about 60–70 c/deg, the regular bars of the interference fringe are no longer visible; observers report a pattern resembling zebra stripes centered on the line of sight. The characteristics of this pattern are consistent with the hypothesis that it is a moiré pattern resulting from aliasing by the foveal cone mosaic. Properties of this moiré pattern allow an assessment of the regularity of the foveal lattice, the spacing between cones, and the light-catching area of individual cones.

Vision receptor    Visual contrast Mosaic    sensitivity Fovea    Retina Laser interferometry    Visual acuity    Visual resolution    Photo-

### INTRODUCTION

It is commonly believed that the optical quality of the human eye is well matched to the spacing of cones at the center of the fovea so that the finest patterns available at the retina are also the finest patterns that the foveal cone mosaic can adequately represent (Snyder and Miller, 1977). Indeed, a number of studies have shown that human visual resolution is not much improved when optical blurring in the eye is reduced with the use of interference fringe stimuli (Le Grand, 1937; Arnulf and Dupuy, 1960; Westheimer, 1960; Campbell and Green, 1965). However, the nature of the limitations on visual resolution imposed by the photoreceptor lattice have not been clearly established experimentally.

The photoreceptor mosaic discretely samples the continuous distribution of light in the retinal image. This renders the visual system, like any discrete imaging system, potentially susceptible to sampling artifacts, or aliasing. The sampling theorem (see Bracewell, 1978) implies that if the regular photoreceptor mosaic is allowed to sample spatial frequencies that are higher than half the reciprocal of the spacing between rows of receptors, the pattern of excitation produced by these frequencies is indistinguishable from a pattern containing low spatial frequencies. That is, if the mosaic is unable to provide at least one row of receptors for each light and each dark bar in the highest spatial frequency in the image, low frequency moiré patterns will intrude, distorting the original image. These patterns are sometimes seen on conventional television screens when patterns such as pin stripes on suits are displayed. In this case, the fundamental frequency of the pin stripe exceeds the lowest frequency that can be adequately represented by the array of phosphor dots on the screen.

If human foveal cones are hexagonally packed, then the critical frequency in c/deg above which

aliasing occurs, the Nyquist limit,  $v_N$ , is

$$v_N = (\sqrt{3}s)^{-1}$$

where  $s$  is the center to center spacing of foveal cones in deg. Osterberg (1935) estimated that the highest density of human foveal cones was  $147,340 \text{ mm}^{-2}$ . Assuming hexagonal packing, this corresponds to a center to center spacing of  $2.8 \mu\text{m}$ . Miller (1979) estimates the closest spacing of human foveal cones to be  $3 \mu\text{m}$ ; we adopt his estimate here. Assuming that  $0.29 \text{ mm}$  on the retina corresponds to  $1 \text{ deg}$  (Hughes, 1977), the minimum foveal cone spacing is about  $0.62 \text{ min of arc}$ , yielding a Nyquist limit of  $56 \text{ c/deg}$ . Estimates of the optical modulation transfer function for the human eye (Campbell and Gubisch, 1966; Van Meeteren, 1974) suggest that the optics reduce the modulation available at the retina by roughly a factor of 10 at this frequency, even under optimal conditions. The optics would render higher spatial frequencies than this even less potent in producing aliasing.

There are additional factors that might preclude aliasing in the fovea. First, irregularity in the mosaic may smear the aliased energy into a broad range of orientations and spatial frequencies, making it less conspicuous (Yellott, 1982). Second, low pass filtering by individual photoreceptors may attenuate high frequency interference fringes that would potentially alias (Miller and Bernard, 1983). Third, fixation instability might produce high temporal frequencies that effectively blur the high spatial frequencies potentially responsible for aliasing.

Ohzu *et al.* (1972) observed moiré patterns when imaging gratings on isolated primate foveal mosaics. Though the exact origin of these patterns is unclear, they suggest that aliasing might be demonstrable psychophysically. There is scant psychophysical evidence for aliasing phenomena in human vision. Hel-

mholtz (1962, Vol. 2, p. 35) noted that fine parallel wires, separated by spaces equal to their width, appeared wavy and distorted when viewed against a bright background. He attributed this distortion to the photoreceptor mosaic. However, the spatial frequencies at which the effect became apparent, 23–25 c/deg. are less than half the foveal Nyquist limit and are therefore too low to produce aliasing in the fovea. Aliasing has been demonstrated psychophysically for the mosaic of short wavelength sensitive cones (Williams *et al.*, 1983a; Williams and Collier, 1983b). The scarcity of these receptors in the human retina (Williams *et al.*, 1981a) allows aliasing to occur at much lower spatial frequencies than would be expected from the foveal mosaic of all three cone types together.

There are several reports in the literature that suggest that foveal aliasing can be observed. Byram (1944) produced a high contrast, retinal interference fringe by viewing a bright line source through a double slit diaphragm. He claimed that 86 c/deg fringes have "a definite wavy appearance and are subject to a rapid shimmering or fluttering movement", attributing this effect to the cone mosaic. These effects were not seen by Westheimer (1960), though they were described by Campbell and Green (1965), using fringes generated with a laser interferometer.

Advances in the control of coherent light have made it possible to construct a laser interferometer that can introduce high frequency, high contrast interference fringes onto the retina without artifact, allowing measurements of contrast sensitivity at spatial frequencies above the resolution limit set largely by the eye's optics under normal viewing conditions. This device allows an objective demonstration of aliasing phenomena in human foveal vision, clarifying the constraints imposed by the photoreceptor mosaic on visual resolution.

#### METHOD

Figure 1 shows a schematic of the interferometer. Beamsplitter,  $BS_1$ , splits light from a 1 mW

helium-neon laser into two beams that follow mirror symmetric but otherwise identical paths. Components for only one path are labelled. Each beam passes through an acousto-optic modulator, AOM, that controls the effective contrast of the interference fringe (see section on Contrast Control). The spatial filter, SF, removes spatial noise from the beam and expands it. It consists of a microscope objective (focal length: 4.3 mm) followed by a 5  $\mu$ m pinhole. After lens,  $L_1$ , collimates the expanded beam, mirror,  $M_1$ , directs the beam onto lens,  $L_2$ , which forms an image of the pinhole inside a glass cube, C. The two beams cross inside the glass cube, travelling in nearly opposite directions, allowing control of the spatial frequency of the interference fringe (see Spatial Frequency Control below). Mirror,  $M_2$ , directs the beam emerging from the glass cube onto collimating lens,  $L_3$ , and then beamsplitter,  $BS_2$ , where the two beams recombine. A circular field stop, FS, defines a 2 deg diameter grating field on the retina. For most observers, the field stop can be sharply focused by adjusting its distance from lens,  $L_4$ . The beamsplitter,  $BS_3$ , allows an auxiliary incoherent field to be added to the grating field. The details of this channel, which has a tungsten halogen source, are not shown. A linear polarizer, oriented so as to transmit the polarized laser output, is placed just before the eye. It attenuates a small amount of depolarized stray light that would otherwise slightly reduce the contrast of the interference fringe.

#### *Vibration isolation and fringe stability*

Interferometers in which the interfering beams have separated optical paths can be vulnerable to fringe instability caused by vibration, which produces variations in the path length difference between the two beams. To reduce this problem, the system is isolated from vibrations transmitted through the floor by floating a vibration-damped optical tabletop on four, six inch diameter inner tubes. The optical paths are folded within each other to minimize the distance between components. Mirrors and beamsplitters are rigidly coupled in pairs so that any path

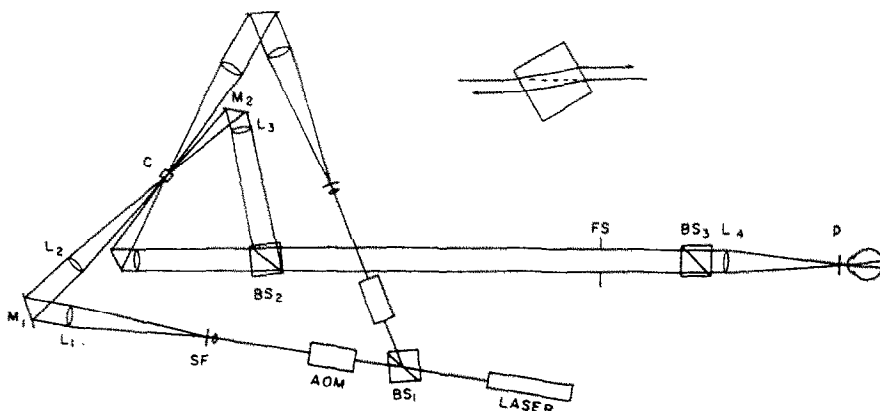


Fig. 1. Schematic of the laser interferometer, with inset showing refraction of light through glass cube, C, that controls fringe spatial frequency.

length variations in one beam will also occur in the other, with the path length difference remaining constant. For example, mirror  $M_1$  of one beam is mounted directly to the same steel platform as mirror  $M_2$  of the opposite beam. These techniques reduce variations in fringe position to less than half a cycle over several seconds, an entirely acceptable level for these experiments.

#### *Spatial frequency control*

The spatial frequency,  $v$ , of an interference fringe is proportional to the separation of the point sources in the entrance pupil

$$v = x/\lambda$$

where  $v$  is given in c/rad,  $\lambda$  is the wavelength of light, and  $x$  is the separation of the point sources in the entrance pupil. Changes in the separation of the point sources must be symmetric with respect to the Stiles-Crawford maximum in the entrance pupil of the eye in order to keep the effectiveness of the beams equal. Symmetric movement in the entrance pupil also helps to avoid the reduction of interference fringe contrast caused by variations in corneal birefringence, since these variations are reported to be radically symmetric about the corneal pole (Bour and Cardozo, 1981).

Suitable manipulation of the glass cube, C, meets this requirement. Consider the inset in Fig. 1, showing the two beams entering the cube from nearly opposite directions. The cube is 25 mm thick and is anti-reflection coated to reduce spurious interference within it. If the beams strike the cube normal to its surface, they pass through unperturbed. However, if the cube lies at a different orientation as shown, each beam is laterally displaced by an amount dependent on the angle of incidence, the refractive index, and the cube thickness. By arranging the beams to pass through the cube in opposite directions, the beams are displaced in opposite directions by the same amount, so that they remain symmetrically positioned in the entrance pupil as spatial frequency is varied. The cube is mounted on a galvanometer motor that can rotate the cube about a horizontal axis nearly orthogonal to the direction of propagation of the beams, producing a vertical displacement of the beams in the entrance pupil and a horizontal interference fringe on the retina.

The experimenter can produce a desired spatial frequency by measuring the separation of an additional image of the point sources identical to that formed in the entrance pupil. This image is formed by a lens identical to  $L_1$  (omitted in Fig. 1 for clarity) that catches the two beams emerging from the other output face of beamsplitter,  $BS_2$ . A narrow slit one focal length from this lens and attached to a micrometer translational stage allows the experimenter to determine the separation of the point sources (and therefore the spatial frequency of the fringe) to within  $10 \mu\text{m}$ . As a check, the spatial frequency was cali-

brated by placing a Ronchi ruling of known spatial frequency (175 c deg) at the field stop, FS. The cube was then rotated until the moiré fringe produced by the interference fringe and the Ronchi ruling had the lowest spatial frequency, since this occurs when the fringe frequency is equal to the fundamental frequency of the ruling. The separation of the point source images at the slit and micrometer agreed with that predicted by the spatial frequency within the error of measurement.

#### *Contrast control*

In order to obtain objective measures of contrast sensitivity with interference fringes, it is desirable to use a forced choice psychophysical procedure. However, this requires the ability to introduce interference fringes into the test field without producing artifacts that might cue the observer that a stimulus has been presented even when the fringe itself is not detected. Therefore, contrast is controlled with a method that keeps the average illumination in the test field, any spatial inhomogeneities in the field (e.g. inevitable dust), and the entry point and polarization of light in the pupil constant throughout fringe presentation. Furthermore, contrast is silently modulated by computer with any desired temporal waveform to which the eye can respond.

The acousto-optic modulator (AOM) in each beam acts as a high speed shutter (see Krauskopf *et al.*, 1981; Wilson and Hawkes, 1983). The rise time measured with a fast photodiode is less than  $0.4 \mu\text{sec}$ . [Acousto-optic modulators alter the wavelength of the transmitted beam depending on the frequency (typically 40 MHz) of the crystal clock that drives them. In order to produce an interference fringe that is stable, it is necessary to drive both modulators from a common crystal clock.] A custom interface controlled by computer gates the modulators, producing a 1 msec rectangular light pulse from each modulator every 2.5 msec (400 Hz). This modulation rate is well above the critical fusion frequency of the eye, so that the observer sees a steady field of light.

The amount of time that the pair of light pulses overlap determines the contrast of the interference fringe. If the pulses arrive at the retina at precisely the same time, they interfere for their entire duration. However, if they fail to overlap at all within the 2.5 msec cycle time, they cannot interfere, and the observer will see nothing but a uniform field of the same average illuminance. The amount of overlap can be controlled in 500, two  $\mu\text{sec}$  steps. Calculations show that the effective contrast of the fringe is given by the overlap of the pulses, expressed as a fraction of the pulse duration.

Figure 2 experimentally confirms this prediction that contrast is a linear function of pulse overlap. Contrast was measured by slowly scanning the interference fringe with a thin slit and photocell at the output of the interferometer. The photocell signal was low-pass filtered to eliminate the high frequencies

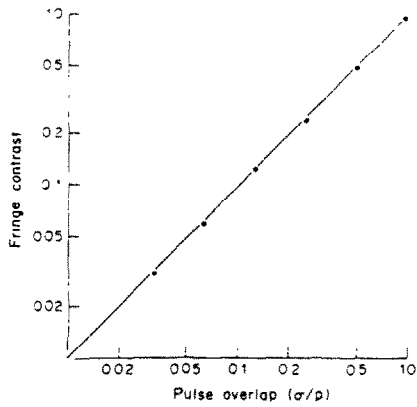


Fig. 2. Contrast of the interference fringe produced by the interferometer, measured with a scanning slit and photocell, as a function of the temporal overlap of the pairs of light pulses in the interfering beams,  $\sigma$ , expressed as a fraction of the pulse duration,  $p$ .

associated with the 400 Hz light pulses, since these are not resolved by the eye. The signal was then displayed on a storage oscilloscope where effective contrast could be measured. When correction is made for the width of the scanning slit, the highest contrast available is not measurably different from unity, suggesting that stray light in the system must be less than about 1%.

#### Alignment procedure

Observers used the following criteria for aligning themselves relative to the point sources in the pupil. Horizontal and vertical alignment criteria involved centering the two point sources relative to the Stiles-Crawford maximum in the entrance pupil. Horizontal alignment was achieved by maximizing the brightness of the field. For vertical alignment, which was a more critical adjustment because of the dependence of fringe contrast on equal effectiveness of the beams, the field stop was temporarily placed in a position that rendered it out of focus and the separation of the point sources was set to roughly 3 mm. This produced a double, but overlapping, image of the field stop. The observer adjusted his vertical position to render the two images of the field stop equally bright.

The observer adjusted the distance of his eye from the final Maxwellian lens to minimize the spatial noise in the field since control experiments showed that spatial noise can seriously degrade contrast sensitivity. Much of this noise arises from inhomogeneities at the cornea. If the cornea lies either in front of or behind the image of the point sources, the field has a granular appearance. This can be reduced by imaging the point sources directly on the cornea, instead of in the plane of the pupil as is common in conventional Maxwellian view. The spatial frequency of the fringe when the point sources are imaged on the corneal surface is negligibly different

from that obtained when they are imaged in the plane of the pupil.

#### Stimulus display and psychophysical procedure

Contrast sensitivity was measured with three observers. Mydriacyl was used to dilate the pupil. For one observer (W.M.), a -4 D correcting lens was placed before the eye, and a small correction was made for the effect of this lens on the spatial frequency of the interference fringe. The test field was 2 deg in diameter, surrounded by an 8 deg annulus formed with incoherent 630 nm light. The radiance of the test field was  $10.2 \log \text{ quanta deg}^{-2} \text{ sec}^{-1}$ . A fixation crosshair visible only in the annulus was centered on the test field. The retinal illuminance of the annulus was adjusted to match that of the test field.

The observer adapted for 30 sec to the stimulus display prior to beginning each run. A two interval forced choice procedure was used to estimate contrast threshold. Two 500 msec intervals, demarcated by tones and separated by 200 msec, were presented on each trial. An interference fringe was presented during only one of the intervals, randomly determined on each trial. The observer's task was to press one of two buttons after each trial, corresponding to the interval containing the fringe. The computer then informed the observer whether or not he was correct via a speech synthesizer. The contrast of the fringe presented on each trial was determined by the maximum likelihood procedure, Quest (Watson and Pelli, 1983). The contrast of the first stimulus was typically set 0.3 log units above the threshold estimated from previous runs. Each threshold estimate is based on 50 trials and represents the 75% frequency of seeing. Runs for which the confidence level that the true threshold lay within plus or minus 0.1 log unit of the estimated threshold was less than 75% were rejected. The value of the slope parameter,  $\beta$ , used in the psychometric function was 3.

A single spatial frequency was presented in each run, and the order in which spatial frequencies were presented was randomized. Owing to the Stiles-Crawford effect, the brightness of the test field depends on the spatial frequency of the fringe. Aside from adjusting the annulus to match the brightness of the test field at each spatial frequency, no attempt was made to compensate for the Stiles-Crawford effect. Four thresholds estimations were obtained in different sessions at each spatial frequency, with all spatial frequencies tested in each session.

The appearance of high frequency interference fringes proved to be a rich source of information. Therefore, in addition to obtaining contrast sensitivity measurements on three observers, 11 observers were aligned in the interferometer and asked to draw or describe the appearance of the fringes at frequencies above 60 c/deg. Observers viewed either a 2 or 4 deg field in which a unity contrast fringe was introduced for 500 msec every 2.5 sec. Two of these

observers were completely naive about the purpose of the experiment and were provided with no information at all about the appearance of the fringes beyond their own observations.

## RESULTS

### *Contrast sensitivity measurements*

Figure 3 shows contrast sensitivity measurements for three observers. Data points represent the mean reciprocal contrast threshold, and error bars represent plus and minus one standard error of the mean based on between-session variability. Contrast sensitivity is maximum at about 10 c/deg. Sensitivity at this frequency is about 50, substantially less than the contrast sensitivities typically obtained (200–300). Control experiments in which 90% of the coherent light is replaced with a steady background of incoherent light yield contrast sensitivity measurements lying in the normal range. This discrepancy is attributed to the fact that the 100% coherent field used in the present experiments inevitably contains spatial noise or speckle that acts as a potent mask, reducing contrast sensitivity.

Contrast sensitivity falls monotonically with increasing spatial frequency but does not reach or even closely approach the abscissa in the neighbourhood of 50–60 c/deg, the classical resolution limit obtained with interference fringes (Westheimer, 1960; Campbell and Green, 1965). Instead, for each observer, the contrast sensitivity function has a broad shoulder that extends well beyond the resolution limit. D.R.W. and M.D. could detect the interval containing the grating at the highest spatial frequencies that could be passed by the dilated pupil (200 c/deg, corresponding to a separation of the point sources in the entrance pupil of 7.25 mm). Observer W.M. could obtain reliable thresholds up to 150 c/deg. In three of the four sessions for this observer, thresholds were

obtained at 170 c/deg but in one session performance was at chance. The next highest frequency tested, 190 c/deg, was too high to be passed by his pupil.

This detection at spatial frequencies higher than the resolution limit of 60 c/deg might suggest an experimental artifact. It may have been, for example, that observers could determine the interval containing the grating on the basis of a detectable transient in the timing of the 400 Hz light pulses in each beam. A control experiment rules this possibility out; if either of the two beams is occluded, no interference fringe can be formed, but the timing of pulses (and therefore any artifact) would be preserved. Under these circumstances, observers never respond better than chance, and no transient can be detected in the field, indicating that detection of these high frequency gratings depends upon simultaneous presentation of the beams and cannot be mediated by any property of either beam alone.

A second possibility was that observers use artifacts associated with the abrupt truncation of the grating by the circular field stop. However, at the higher spatial frequencies employed, these truncation artifacts are extremely small. Furthermore, when the fringes are windowed with an aperture producing a smooth Gaussian envelope, the ability to detect these gratings is preserved. Since the interferometer allows the introduction of fringes into the stimulus field without changing the entry point or polarization of light in the pupil, these factors cannot account for the detectability of these fringes.

### *The appearance of high frequency interference fringes*

The descriptions of the appearance of interference fringes whose spatial frequency exceeds 60 c/deg are similar across all 11 observers. The drawings and verbal reports provided by the two naive observers were essentially the same as those of the other

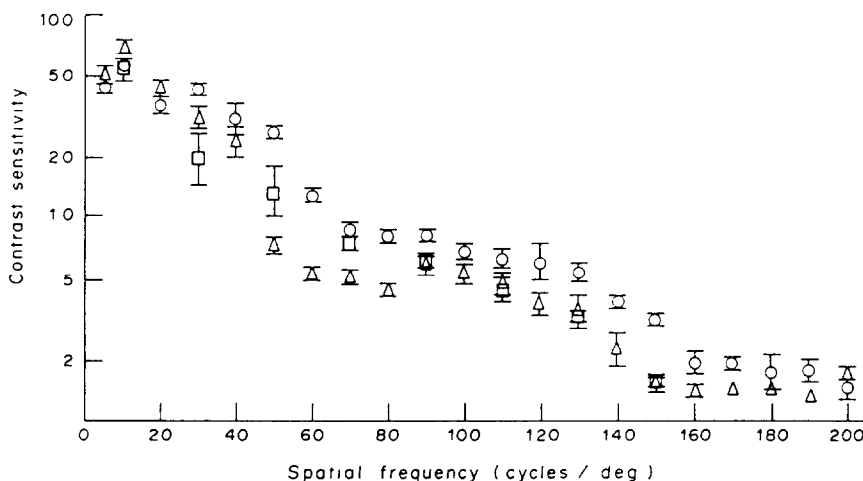


Fig. 3. Contrast sensitivity (reciprocal threshold contrast) for three observers as a function of spatial frequency. Circles, D.R.W.; Squares, W.M.; Triangles, M.D. Error bars represent plus and minus one standard error of the mean based on variability between four sessions. 2 deg field centrally fixated, 632.8 nm, 10.2 log quanta  $\text{deg}^{-2} \text{sec}^{-1}$ .

observers. These reports also concur with those of Byram (1944) and Campbell and Green (1965), although there are several features of the present description that they did not describe.

In the range between 0 and 45 c/deg or so, the interference fringe can be seen across the entire field. The introduction of the fringe into the field is accompanied by a desaturation and yellowing of the whole field, as reported by Campbell and Green (1965). As spatial frequency increases from about 45 c/deg, the bars of the fringe can be seen only in a progressively smaller region of the field that moves with the eye and is centered on the line of sight.

At roughly 60 c/deg, the fine, regular bars are lost in the spatial noise that characterizes coherent fields. However, the fringe presentation is still readily detectable because of the desaturation and yellowing of the field, which is now confined to the central 3 deg or so of the fovea. The origin of the desaturation and yellowing of the test field when the fringe is introduced reflects a nonlinearity in the visual system that may be related to effects described by Burton (1973). It may also be related to the changes in hue reported when fields of light are temporally modulated (Inglis and Martinez-Urieegas, 1983). At 60 c/deg and retinal eccentricities beyond the central 3 deg of the fovea, some observers report a faint granular appearance of the field, resembling non-oriented, two-dimensional noise. Also, most observers report the appearance of an annulus of extremely fine wavy lines whose diameter is roughly 2.5 deg, centred on the line of sight. A drawing made by the author depicting the appearance of the annulus at 80 c/deg is shown in Fig. 4(a).

As spatial frequency increases, this annulus of wavy lines shrinks, finally collapsing to a circular patch at a frequency of 90–100 c/deg. Observers describe this patch as resembling a fingerprint or pattern of zebra stripes. Figure 4(b) and (c) show drawings of the appearance of a 110 c/deg interference fringe made by the author and a naive observer, respectively. The scale bar in the drawing represents 1 deg visual angle.

The zebra stripes maintain a fixed configuration at a given spatial frequency and drawings made of them weeks apart reveal the same pattern. The pattern does not depend on the entry point of the point sources (at a fixed separation) in the pupil, except that its visibility is reduced when the point sources are asymmetrically placed relative to the Stiles–Crawford maximum. The pattern is small and scintillates markedly. This, coupled with the presence of spatial noise in the coherent field, make it difficult to characterize the spatial structure in the field with precision.

Between 100 and 150 c/deg, the patch of zebra stripes diminishes in size. Between 150 and 160 c/deg, the zebra stripe pattern disappears abruptly. At higher frequencies up to the limit (about 200 c/deg) set by the diameter of the pupil, the interference fringe can only be detected by a faint, scintillating,

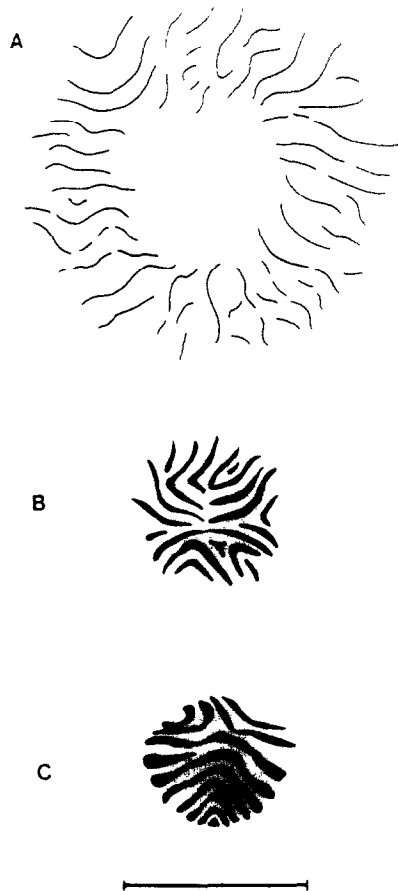


Fig. 4. (a) Author's drawing of the appearance of an 80 c/deg interference fringe. (b) Author's drawing of the appearance of a 110 c/deg interference fringe. (c) Drawing made by a naive observer of a 110 c/deg interference fringe. Scale bar at bottom corresponds to 1 deg visual angle.

granular appearance of the field within the central fovea.

#### DISCUSSION

The most likely explanation for the zebra stripes is that they represent a moiré fringe resulting from undersampling (aliasing) by the photoreceptor mosaic. Figure 5 shows a tangential section through the central fovea of *Macaca fascicularis*. The specimen was prepared by William Miller. The regularity of the array of cones is readily apparent (Hirsch and Hylton, 1984), despite a histological artifact running through the center of the specimen. In order to compare the anatomical data from the monkey with the psychophysical observations from humans, correction must be made for differences in photoreceptor spacing and posterior nodal distance. These differences imply that the monkey foveal Nyquist limit is 50 c/deg instead of 56 as in man (Miller, 1979). Under the assumption that these are the only relevant differences between the eyes of monkey and man, a comparison can be made by scaling the angular dimensions of the monkey anatomy by the ratio of

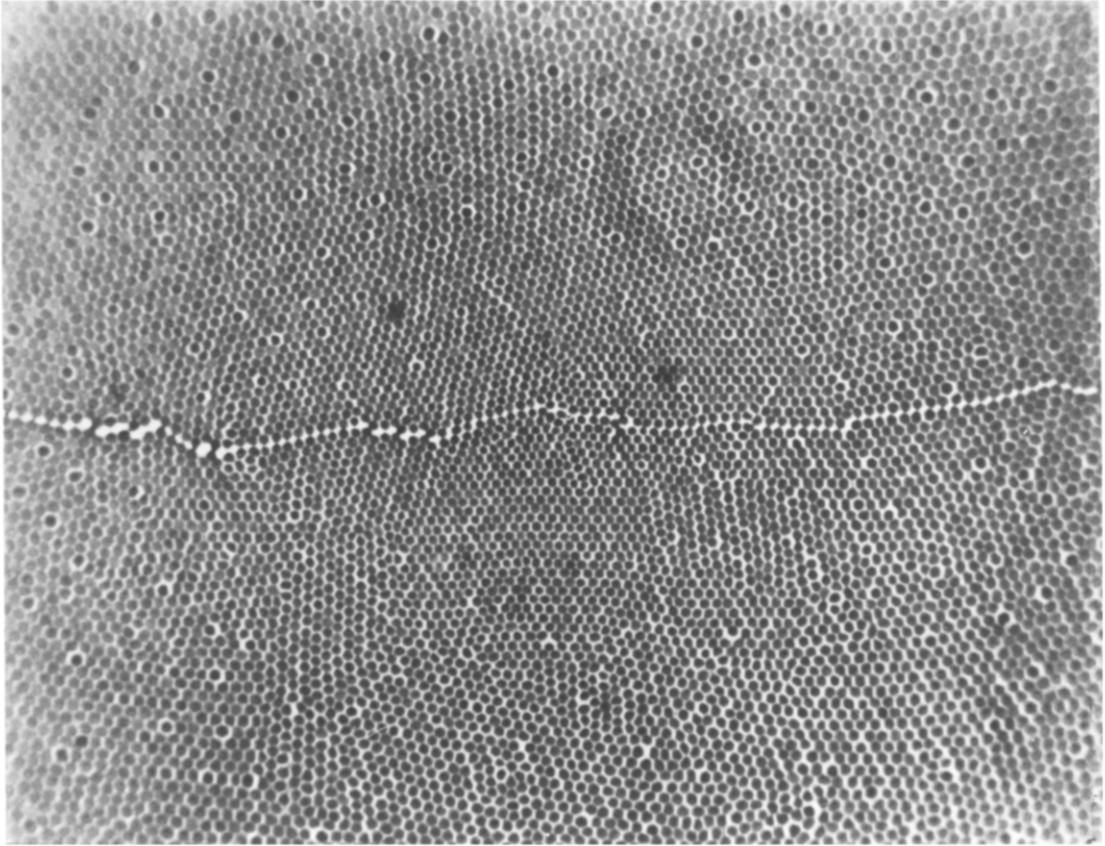
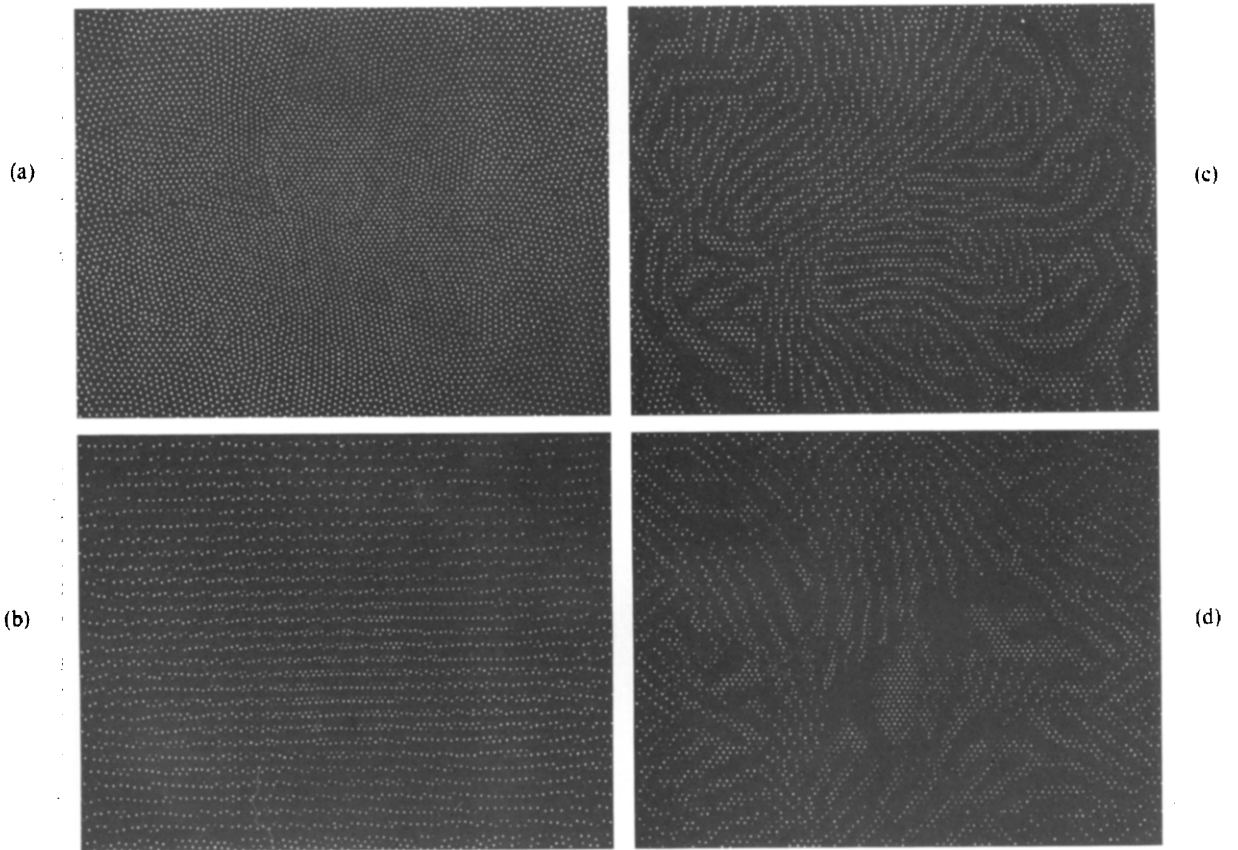


Fig. 5. Tangential section made at the external limiting membrane through the central fovea of *Macaca fascicularis*. Specimen was prepared by William Miller. Width of image would correspond to about 1 deg visual angle in the human.



**Fig. 6.** (a) Mosaic is 5(a) reduced to a series of points, each point corresponding to the location of a single foveal cone. (b) Dot foveal mosaic sandwiched with a 40 c/deg square wave grating. (c) Mosaic sandwiched with an 80 c/deg square wave grating. (d) Mosaic sandwiched with a 110 c/deg square wave grating.

the Nyquist limits. The width of the tangential section shown here would then correspond to roughly the central one deg of the human fovea.

The sampling properties of this mosaic can be revealed with the technique developed by Yellott (1982): Fig. 6(a) shows the same mosaic, reduced to a series of points, with each point marking the center of an individual cone. Figure 6(b) shows the consequences of imaging a 40 c/deg grating on the mosaic: the mosaic can portray the grating with little distortion. However, Fig. 6(c) shows the consequences of sampling an 80 c/deg grating, which is well above the Nyquist limit of about 56 c/deg. A moiré pattern of wavy stripes is formed whose characteristics match the appearance of an 80 c/deg interference fringe [see Fig. 4(a)]. The spatial frequency of the moiré is high at the foveal center, roughly 30–35 c/deg, and would presumably be difficult to see. However, the moiré frequency declines with eccentricity as the cone spacing more nearly matches the period of the grating. At larger eccentricities, beyond those shown in this specimen, the spatial frequency would presumably increase again as the cone spacing and grating period become mismatched again. Presumably, a larger view of the mosaic would reveal the annular ring of moiré fringes described by observers viewing 80 c/deg fringes. Figure 6(d) shows the moiré produced by a 110 c/deg fringe, whose period is close to the spacing of rows of receptors at the very center of the fovea, that is, close to twice the Nyquist limit. In this case, the moiré is coarsest at the center, becoming finer with increasing eccentricity. This is also consistent with the subjective reports of the observers [see Fig. 4(b) and (c)].

#### *Foveal cone spacing*

If the zebra stripes actually result from aliasing by foveal cones, then there must be quantitative agreement between anatomical estimates of cone spacing, fringe spatial frequency, and the resulting moiré pattern. Moiré patterns have the lowest spatial frequency when the spacing of elements in the two patterns producing the moiré is the same. Thus, the zebra stripes should have the lowest spatial frequency when the period of the interference fringe equals the spacing of rows of foveal cones. Three observers (D.R.W., M.D. and R.S.) adjusted the spatial frequency of a horizontal interference fringe so that the zebra stripes on the line of sight appeared coarsest.

The spatial frequencies set by the observers were 119, 109 and 105 c/deg respectively, corresponding to fringe periods of 0.50, 0.55 and 0.57 min of arc (with standard errors of the mean of 0.007, 0.008 and 0.016 based on four settings). This agrees quite well with the spacing of rows of receptors at the foveal center, which is 0.54 min of arc ( $\sqrt{3}/2$  times the center to center spacing of 0.62 min of arc assuming a hexagonal lattice)\*.

The quantitative agreement between the characteristics of the zebra stripes and anatomical estimates of cone spacing supports the hypothesis that the zebra stripes result from aliasing by the cone mosaic. It also tends to rule out the hypothesis that the zebra stripe pattern is generated by aliasing at a later stage in the visual pathway than the photoreceptor mosaic. Post-receptoral aliasing could conceivably occur if, for example, the array of ganglion cells mediating foveal vision had a lower sampling rate than the cones themselves. Then, the spatial frequencies producing the coarsest moiré patterns could be lower than those that are optimal for the cone mosaic, but this is not observed in the central fovea at least.

Low frequency moiré patterns introduced into the visual system by photoreceptor aliasing are unlikely to be selectively attenuated by later stages of processing. That is, low-pass filtering that might result from pooling cone signals or electrical coupling between cones will attenuate low frequency signals actually present in the image and low frequency aliases of high frequencies equally.

#### *Regularity of the foveal lattice*

The regularity of the foveal cone mosaic is reflected in the regularity of the moiré pattern it produces with a sinusoidal grating: regular lattices produce regular moiré patterns while irregular lattices produce irregular moiré patterns. Williams and Collier (1983) and Williams *et al.* (1983) showed that the mosaic of short wavelength cones produces detectable aliasing energy that is broadly tuned in orientation and spatial frequency, resembling two-dimensional noise. This is consistent with anatomical evidence for an irregular (though nonrandom) pattern of short wavelength cones (De Monasterio *et al.*, 1981; and Williams *et al.*, 1983) in the primate.

The human fovea, on the other hand, appears to have a much more regular lattice, since the moiré pattern it produces is much more regular. The sketches made by observers viewing high frequency fringes are probably too uncertain to justify a quantitative evaluation of lattice regularity. However, it is clear that observers can see curved stripes extending over distances of more than 30 min of arc, and this suggests a high degree of local regularity. This is consistent with the best anatomical evidence on primate lattice quality (Borwein *et al.*, 1980; Hirsch and Hylton, 1983; Miller, 1979; Osterberg, 1935).

This psychophysical evidence for a regular lattice of human foveal cones shows that the visual system

\*The fringe period that will produce the lowest frequency moiré pattern depends slightly on the orientation of the fringe relative to the mosaic. This dependence will be described in a later publication. The wavy nature of the zebra stripes suggests that the orientation of the lattice changes within the fovea. The 632.8 nm light used in these observations will stimulate both the red and green sensitive cones, but not the blue sensitive cones. We neglect them here since they are too rare in the central fovea to substantively alter the results (Williams *et al.*, 1981b).

has not attempted to exploit irregularity in the mosaic as a way of reducing the conspicuousness of foveal aliasing. This should not be too surprising in light of the protective effect afforded by optical blurring. This allows hexagonally packed elements to fill the retinal surface with minimal gaps between them, maximizing quantum catching efficiency. At the same time, hexagonal packing minimizes orientational anisotropy and the number of receptors per unit retinal area required to achieve a given Nyquist limit.

Lattice quality diminishes rapidly with retinal eccentricity: as rods begin to intrude, the cone lattice becomes irregular but nonrandom (Borwein *et al.*, 1980). This is consistent with the psychophysical observations, since the largest annulus of zebra stripes has a diameter of roughly 2.5 deg (at about 60 c/deg). At lower spatial frequencies, still too high for the eccentric retina to resolve in the usual sense, some observers report a faint granular appearance of the field. This may represent the nonoriented, broadband noise expected from under-sampling by an irregular mosaic (Yellott, 1982; Yellott, 1983; Williams and Collier, 1983; Williams *et al.*, 1983). However, other alternatives, such as that moiré patterns are produced with the retinal vasculature, have not been excluded. The vasculature cannot account for the zebra stripes seen in the central fovea since no blood vessels exist there (Polyak, 1941).

#### *Integration area of single foveal cones*

Low pass filtering prior to sampling by the photoreceptor mosaic will attenuate high spatial frequencies that would potentially alias. The finite size of individual cones acts as a low pass filter in addition to the filtering performed by the optics of the eye (Snyder and Miller, 1977; Miller and Bernard, 1983). We adopt the simplifying assumption that the effectiveness of a quantum is independent of its entry point in the receptor aperture provided that it falls within some critical radius of the receptor axis, and that it is ineffective if it falls outside this radius. That is, we assume that the integration area of a foveal cone can be adequately described by a cylinder function.\* The modulation transfer function,  $M$ , for such an aperture is a damped first order Bessel function given by

$$M = 2J_1(\pi v A) / (\pi v A)$$

where  $J_1$  is a Bessel function,  $v$  is spatial frequency, and  $A$  is the diameter of the foveal cone aperture (Miller and Bernard, 1983). The function predicts that the alias of a high frequency interference fringe should not be visible when the frequency of the fringe equals the first zero crossing of the aperture modulation transfer function.

Observers M.D., D.R.W. and W.M. reported that the zebra stripe pattern is continuously visible in the range between 60 and 150–160 c/deg, at which point it abruptly vanishes at the foveal center. At higher spatial frequencies, fringes can be detected on the basis of a granular appearance of the field near fixation. The origin of this percept is unclear and observations at these high frequencies are hampered by increasing spatial noise in the field, presumably caused by irregularities in the paraxial optics of the eye. Still, foveal aliasing is clearly visible up to 150 c/deg, in agreement with the observations of Byram (1944), and this provides a lower limit on the frequency corresponding to the first zero crossing of the cone MTF and an upper limit on the effective diameter of a central foveal cone. Under these assumptions, the diameter of the cone aperture cannot exceed 2.3  $\mu\text{m}$ , or 77% of the minimum center-to-center cone spacing. This suggests that optical cross-talk between foveal cones is quite small. The present evidence cannot rule out a smaller aperture than this, since other factors such as stray light and eye tremor may also selectively reduce the detectability of these very high frequency fringes. However, the value of 2.3  $\mu\text{m}$  is independently supported by light microscopic observations made by Miller and Bernard (1983).

Laser interferometry can produce sinusoidal gratings on the retina of substantially higher contrast than can conventional incoherent viewing because the light is constrained to pass through two tiny portions of the eye's optics. Aberrations produced by large scale variations in optical power are avoided because these simply produce a phase shift in the fringe rather than a reduction in contrast (Saleh, 1982). However, interferometry is not immune to "local aberrations": light-scattering inhomogeneities in the optics and retina can reduce fringe contrast. Neither the amount of light scattered under these conditions, nor its dependence on spatial frequency have been well determined. However, the demonstration of fringe detection at frequencies as high as 200 c/deg suggests that the attenuation attributable to scatter cannot depend strongly on spatial frequency. It also shows that eye movements are not sufficient to eliminate aliasing, though they may reduce its visibility. The scintillation of the field at the line of sight seen when viewing these high frequency fringes is probably the result of eye movements. Simulations of eye movements made by moving gratings relative to the monkey foveal mosaic mimic this scintillation well.

In the fovea, at least, the most important factor in reducing the visibility of aliasing is optical blurring. Other factors presumably become more important in the near peripheral retina where cone spacing is larger and optical quality little changed. When optical attenuation is largely removed, aliasing phenomena can be observed with an interference fringe whose contrast is on the order of 20% at 110 c/deg, in spite of eye tremor and stray light.

\*Functions for which the effectiveness of a quantum falls off smoothly with eccentricity in the aperture, such as a Gaussian, might be more realistic, but will not grossly change the results of this analysis.

The appearance of foveal aliasing phenomena at spatial frequencies above the highest typically transferred by the optics of the eye confirms the hypothesis that the optics and mosaic are roughly matched. When optical blurring is reduced with laser interferometry, aliasing by the cone mosaic ultimately limits human visual resolution.

*Acknowledgements*—I am grateful for discussions with Dan Green, Joy Hirsch, Walt Makous, William Miller, John Krauskopf, Denis Pelli and Jack Yellott. I also thank William Miller for providing the monkey mosaic, and Dave Kurtz, Bill Vaughn and Larry Ota for their help in constructing the interferometer. Supported by EY01319 and EY04367A.

#### REFERENCES

- Arnulf A. and Dupuy O. (1960) La transmission des contrastes par le système optique de l'oeil et les seuils des contrastes rétinien. *C.r. Acad. Sci., Paris* **250**, 2757–2759.
- Borwein B., Borwein D., Medeiros J. and McGowan J. W. (1980) The ultrastructure of monkey foveal photoreceptors, with special reference to the structure, shape, size and spacing of the foveal cones. *Am. J. Anat.* **159**, 125–146.
- Bour L. J. and Cardozo N. J. L. (1981) On the birefringence of the living human eye. *Vision Res.* **21**, 1413–1421.
- Bracewell R. N. (1978) *The Fourier Transform and Its Applications*. McGraw-Hill, New York.
- Burton G. J. (1973) Evidence for non-linear response processes in the human visual system from measurements on the thresholds of spatial beat frequencies. *Vision Res.* **13**, 1211–1225.
- Byram G. M. (1944) The physical and photochemical basis of visual resolving power. Part II. Visual acuity and the photochemistry of the retina. *J. opt. Soc. Am.* **34**, 718–738.
- Campbell F. W. and Green D. G. (1965) Optical and retinal factors affecting visual resolution. *J. Physiol.* **181**, 576–593.
- Campbell F. W. and Gubisch R. W. (1966) Optical quality of the human eye. *J. Physiol.* **186**, 558–578.
- de Monasterio F. M., Schein S. J. and McCrane E. P. (1981) Staining of blue-sensitive cones of the macaque retina by a fluorescent dye. *Science* **213**, 1278–1281.
- Helmholtz H. (1962) *Helmholtz's Treatise on Physiological Optics* (Edited by Southall J. P. C.). 3rd edn. Dover, New York.
- Hirsch J. and Hylton R. (1984) Quality of the primate photoreceptor lattice and limits of spatial vision. *Vision Res.* **24**, 347–356.
- Hughes A. (1977) The topography of vision in mammals of contrasting life style: comparative optics and retinal organisation. In *Handbook of Sensory Physiology*, pp. 613–756. Springer, Berlin.
- Ingling C. R. Jr. and Martinez-Uriegas E. (1983) Simple-opponent receptive fields are asymmetrical: G-cone centers predominate. *J. opt. Soc. Am.* **73**, 1527–1532.
- Krauskopf J., Williams D. R. and Heeley D. W. (1981) Computer controlled color mixer with laser primaries. *Vision Res.* **21**, 951–953.
- Le Grand Y. (1937) La formation des images rétinien. Sur un mode de vision éliminant les défauts optiques de l'oeil. *2e Reunion de l'Institute d'Optique*, Paris.
- Miller W. H. (1979) Ocular optical filtering. In *Handbook of Sensory Physiology*. Springer, Berlin.
- Miller W. H. and Bernard G. D. (1983) Averaging over the foveal receptor aperture curtails aliasing. *Vision Res.* **23**, 1365–1369.
- Ohzu H., Enoch J. M. and O'Hair J. C. (1972) Optical modulation by the isolated retina and retinal receptors. *Vision Res.* **12**, 231–244.
- Osterberg G. (1935) Topography of the layer of rods and cones in the human retina. *Acta Ophthal., Suppl.* **6**, 1–103.
- Polyak S. (1941) *The Retina*. Univ. of Chicago Press.
- Saleh B. E. A. (1982) Optical information processing and the human visual system. In *Applications of Optical Fourier Transforms*, pp. 431–465. Academic Press, New York.
- Snyder A. W. and Miller W. H. (1977) Photoreceptor diameter and spacing for highest resolving power. *J. opt. Soc. Am.* **67**, 696–698.
- van Meeteren A. (1974) Calculations on the optical modulation transfer function of the human eye for white light. *Optica Acta* **21**, 395–412.
- Watson A. B. and Pelli D. G. (1983) QUEST: A Bayesian adaptive psychometric method. *Percept. Psychophys.* **33**, 113–120.
- Westheimer G. (1960) Modulation thresholds for sinusoidal light distributions on the retina. *J. Physiol.* **152**, 67–74.
- Williams D. R. and Collier R. J. (1983) Consequences of spatial sampling by a human photoreceptor mosaic. *Science* **221**, 385–387.
- Williams D. R., Collier R. J. and Thompson B. J. (1983) Spatial resolution of the short-wavelength mechanism. In *Colour Vision*, pp. 487–503. Academic Press, New York.
- Williams D. R., MacLeod D. I. A. and Hayhoe M. M. (1981a) Punctate sensitivity of the blue-sensitive mechanism. *Vision Res.* **21**, 1357–1375.
- Williams D. R., MacLeod D. I. A. and Hayhoe M. M. (1981b) Foveal tritanopia. *Vision Res.* **21**, 1341–1356.
- Wilson J. and Hawkes J. F. B. (1983) *Optoelectronics: An Introduction*. Prentice-Hall, NJ.
- Yellott J. I. Jr. (1982) Spectral analysis of spatial sampling by photoreceptors: Topological disorder prevents aliasing. *Vision Res.* **22**, 1205–1210.
- Yellott J. I. Jr. (1983) Spectral consequences of photoreceptor sampling in the rhesus retina. *Science* **221**, 382–385.